Electromagnetic diffraction by two perfectly conducting wedges with dented edges loaded with a dielectric cylinder

A.Z. Elsherbeni, PhD
H.A. Auda, PhD

Indexing terms: Electromagnetic theory, Numerical analysis

Abstract: A rigorous field analysis of the problem of two identical perfectly conducting parallel wedges with dented edges loaded with a dielectric cylinder, and excited by an electric or magnetic line current in the upper sector, is given in this paper. The dielectric medium is assumed to be linear, homogeneous, isotropic and free from losses, whereas the mediums of the upper and lower sectors are free space. A field equivalence theorem is used to derive, for each excitation, a system of coupled integral equations for the equivalent magnetic currents on the dielectric interfaces, which is later solved using Galerkin's method. The fields and powers transmitted into the lower sector, hence the transmission coefficients, for both polarisations are subsequently determined in terms of the equivalent magnetic currents on the lower dielectric interface. The analysis is then specialised to the problem of a slit loaded with a dielectric cylinder, as well as to the case of plane wave excitation. Sample numerical results for the dielectric-loaded double dented wedge and slit problems in the case of plane wave excitation are also given.

1 Introduction

The problem of a line source radiating in the presence of a perfectly conducting wedge is a classical problem in electromagnetic field theory. Both the wedge geometry and its generalisation to two perfectly conducting parallel wedges, i.e. wedges of parallel axes are actually encountered in a variety of engineering applications because of their canonical structures. A closed form solution of the single wedge problem in the form of an infinite series is possible due to the separability of the Helmholtz wave equation for the wedge geometry in cylindrical coordinates [Reference 1 Section 5.10]. On the other hand, the closed-form solution of the double wedge problem is not possible, except for the special cases of the flanged parallel-plate waveguide [2, 3] and the slit [4]. Previous investigations have therefore almost exclusively relied on approximate techniques for the solution of this problem. Teague and Zitron [5] obtained an asymptotic representation of the diffracted field using the approximation of the scattering by two bodies given by Zitron and Karp [6]. The double wedge problem has also been solved asymptotically for an incident E-polarised plane wave by Elsherbeni and Hamid [7] using an approximate technique developed by Karp and Russek [8] for the diffraction by a wide slit, and very recently, using the cylindrical-wave spectrum technique [9]. In addition, they studied the effect on the transmission coefficient due to rounded and capped edges and in the presence of a perfectly conducting or dielectric cylinder asymptotically in References 10 through 12, and due to truncated edges using a hybrid numerical technique in Reference 13.

In this paper, a rigorous field analysis of the problem of diffraction of electromagnetic waves by two similar perfectly conducting parallel wedges with dented edges is presented. The wedges are loaded with a dielectric cylinder whose circumference coincides with the circular arcs of the dents, as is shown in Fig. 1. The axis of the cylinder is therefore the line of intersection of the two similar wedges. Furthermore, the dielectric medium is assumed to be linear, homogeneous, isotropic and free from losses, and is therefore characterised by the real scalars permittivity ε, permeability μ, and wave number κ. The mediums of the upper and lower sectors are free spaces whose constitutive parameters are ε_0, μ_0 and κ_0. In view of the two-dimensional character of the problem, the analysis is carried out for the transverse electric (TE) and magnetic (TM) to z excitations separately. The sources in the TE and TM cases are, respectively, magnetic and electric line currents located in the upper sector.

The analysis is based on applying a field equivalence theorem to divide the problem into three problems for the upper and lower sectors and dielectric cylinder for each excitation. The fields in the equivalent problem for

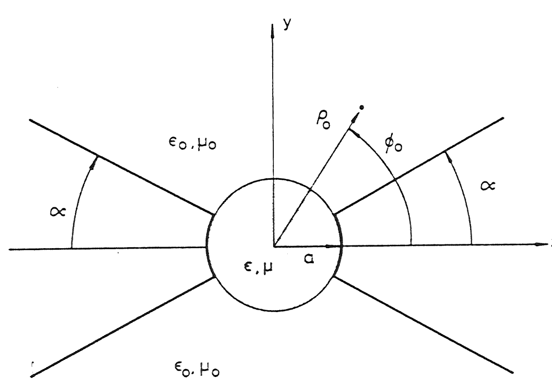

Fig. 1 *Two parallel perfectly conducting wedges with dented edges loaded with dielectric cylinder*

Paper 6618H (E11), first received 11th August 1988 and in revised form 18th January 1989

The authors are with the Department of Electrical Engineering, University of Mississippi, University, Mississippi 38677, USA

the upper sector are produced by the line current source and equivalent magnetic currents placed on the dielectric interface while it is short-circuited, i.e. covered with a perfect electric conductor. The fields in the equivalent problem for the lower sector are produced by equivalent magnetic currents placed on the dielectric interface while it is short-circuited. The fields in the equivalent problem for the dielectric cylinder are produced by the negatives of the magnetic currents in the equivalent problems for the upper and lower sectors placed on the dielectric interfaces while they are short-circuited. The tangential components of the electric field at the perfectly conducting wedges do vanish in this procedure by construction, and are continuous across the dielectric interfaces by virtue of the proper choice of magnetic currents placed on the opposite sides of the short-circuited dielectric interfaces. Enforcing the continuity of the tangential components of magnetic field across these interfaces then results in a system of two coupled integral equations for the equivalent magnetic currents. The solution of this system of integral equations is carried out using Galerkin's method. The field and power transmitted into the lower sector, and hence the transmission coefficient, are subsequently determined in terms of the equivalent magnetic currents on the lower dielectric interface. Finally, the analysis is specialised to the problem of a slit loaded with a dielectric cylinder shown in Fig. 2, as well as to the case of plane wave excitation. Sample numerical results in the case of plane wave excitation are also given.

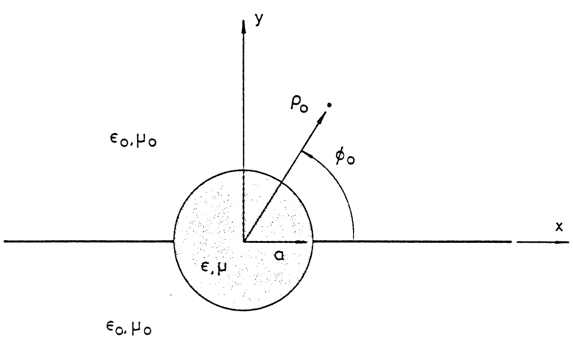

Fig. 2 *Slit in perfectly conducting plane loaded with dielectric cylinder*

2 Basic formulation

Let the excitation of the dielectric-loaded double dented wedge be a line current located in the upper sector at $\rho = \rho_0$ and $\phi = \phi_0$. The analysis can be specialised for plane wave excitation by letting the line current recede to infinity.

The total field, incident plus scattered, must have zero electric field components tangent to the perfectly conducting wedges and continuous tangential electric and magnetic fields across the dielectric interfaces. A field equivalence theorem is used to divide the problem into three problems for the upper and lower sectors and the dielectric cylinder as follows. Let the exciting field be the field produced by the line current while the dielectric interfaces are short-circuited, i.e. covered with perfect electric conductors. This field, often referred to as the short-circuit field, is denoted (E^{sc}, H^{sc}). Furthermore, let $(E^u(M_1), H^u(M_1))$, and $(E^d(-M_1), H^d(-M_1))$ be, respectively, the fields produced in the upper sector and inside the dielectric cylinder by the magnetic current sheet

$$M_1 = E_1 \times a_\rho \tag{1}$$

on the dielectric interface $\rho = a$, $\pi - \alpha \geqslant \phi \geqslant \alpha$, and let $(E^l(M_2), H^l(M_2))$ and $(E^d(-M_2), H^d(-M_2))$ be, respectively, the fields produced in the lower sector and inside the dielectric cylinder by the magnetic current sheet

$$M_2 = E_2 \times a_\rho \tag{2}$$

on the dielectric interface $\rho = a$, $-\alpha \geqslant \phi \geqslant \alpha - \pi$, while they are short-circuited. In eqns. 1 and 2, E_1 and E_2 are the total electric fields on the corresponding interfaces. According to the field equivalence theorem [Reference 1, Section 3.5], the total field in the upper sector is identical to $(E^{sc} + E^u(M_1), H^{sc} + H^u(M_1))$, the field in the dielectric cylinder is identical to $(-E^d(M_1 + M_2), -H^d(M_1 + M_2))$, whereas the field in the lower sector is identical to $(E^l(M_2), H^l(M_2))$. The equivalent situations are shown in Fig. 3.

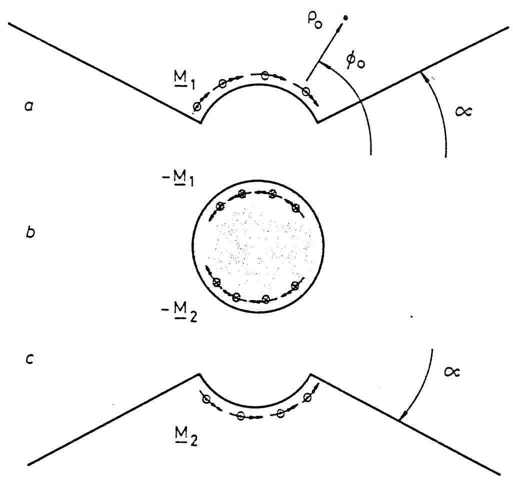

Fig. 3 *Equivalent situations*
a Equivalence for upper sector
b Equivalence for dielectric cylinder
c Equivalence for lower sector

The tangential components of the electric field do vanish at the perfectly conducting wedges by construction, and are continuous across the dielectric interfaces by virtue of placing magnetic current sheets of equal amplitudes and opposite signs on the opposite sides of the short-circuited interfaces. The continuity of the tangential components of the magnetic field across the interfaces, however, requires that

$$a_\rho \times (H^u(M_1) + H^d(M_1 + M_2)) = -a_\rho \times H^{sc} \qquad \rho = a,\ \pi - \alpha \geqslant \phi \geqslant \alpha \tag{3}$$

$$a_\rho \times (H^l(M_2) + H^d(M_1 + M_2)) = 0 \qquad \rho = a,\ -\alpha \geqslant \phi \geqslant \alpha - \pi \tag{4}$$

which are a coupled pair of equations to be solved for the equivalent magnetic currents M_1 and M_2.

3 TE excitation

The source for the TE excitation is a magnetic line current of unit amplitude. The field produced by this current source can only have a z-component of magnetic field that does not vary with z and no such component of electric field. It then follows from eqns. 1 and 2 that the equivalent magnetic currents have only a z-component that does not vary with z, i.e.

$$M^h_{1,2} = M^h_{1,2}(\phi')a_z \tag{5}$$

where primed co-ordinates are used to locate source points.

Thus, all the sources involved in the equivalent problems are z-directed distributions of uniform magnetic line currents. The magnetic field in any of the equivalent problems can then be derived from a z-directed electric vector potential $F = F_z(\rho, \phi)a_z$ as [Reference 1 Section 5.1]

$$H_z = -j\omega\varepsilon_0 \varepsilon_r F_z(\rho, \phi) \tag{6}$$

where the dielectric constant ε_r is unity in the equivalent problems for the upper and lower sectors, and is an arbitrary real scalar in the equivalent problem for the dielectric cylinder. Consequently, the z-components of the electric vector potentials in the equivalent problems can be determined in terms of the magnetic Green's functions Γ^{cw} of a capped wedge of half-angle $0.5\pi + \alpha$ and Γ^{wg} of a cylindrical waveguide as

$$F_z^{sc}(\rho, \phi) = \Gamma^{cw}(\rho_0, \phi_0 \,|\, \rho, \phi) \tag{7}$$

$$F_z^{u}(\rho, \phi) = a \int_{\alpha}^{\pi-\alpha} M_1^h(\phi')\Gamma^{cw}(\rho, \phi \,|\, a, \phi')\, d\phi' \tag{8}$$

$$F_z^{d}(\rho, \phi) = -a\left(\int_{\alpha}^{\pi-\alpha} M_1^h(\phi')\Gamma^{wg}(\rho, \phi \,|\, a, \phi')\, d\phi' + \int_{\alpha-\pi}^{-\alpha} M_2^h(\phi')\Gamma^{wg}(\rho, \phi \,|\, a, \phi')\, d\phi'\right) \tag{9}$$

$$F_z^{l}(\rho, \phi) = a \int_{\alpha-\pi}^{-\alpha} M_2^h(\phi')\Gamma^{cw}(\rho, \phi \,|\, a, \phi')\, d\phi' \tag{10}$$

where

$$\Gamma^{cw}(\rho, \phi \,|\, \rho', \phi') = j\frac{\psi(\alpha)}{2}\sum_{n=0}^{\infty} v_n H_{n\psi(\alpha)}^{(2)}(\kappa_0 \rho) \times \left(H_{n\psi(\alpha)}^{(2)}(\kappa_0 \rho')\frac{J'_{n\psi(\alpha)}(\kappa_0 a)}{H_{n\psi(\alpha)}^{(2)\prime}(\kappa_0 a)} - J_{n\psi(\alpha)}(\kappa_0 \rho')\right) \times \cos n\psi(\alpha)(\phi \mp \alpha)\cos n\psi(\alpha)(\phi' \mp \alpha) \quad \rho \geqslant \rho' \tag{11}$$

$$\Gamma^{wg}(\rho, \phi \,|\, \rho', \phi') = \frac{1}{j4}\sum_{n=0}^{\infty} v_n J_n(\kappa\rho) \times \left(H_n^{(2)}(\kappa\rho') - \frac{H_n^{(2)\prime}(\kappa a)}{J'_n(\kappa a)} J_n(\kappa\rho')\right) \times \cos n(\phi - \phi') \quad \rho' \geqslant \rho \tag{12}$$

In eqns. 11 and 12, $H^{(2)}$ and J are, respectively, the Hankel function of the second kind and Bessel function of the first kind, primes denote derivatives of the functions with respect to their arguments, and v_n is the Neumann's number (where $v_0 = 1$, and $v_n = 2$ for $n \geqslant 1$). Furthermore, the Hankel and Bessel functions in eqn. 12 are of integral order n, whereas the order of these functions in eqn. 11 is n times $\psi(\alpha)$, where

$$\psi(\alpha) = \frac{\pi}{\pi - 2\alpha} \tag{13}$$

Finally, the minus and plus signs in eqn. 11 correspond, respectively, to the upper and lower sectors. It is worth noting that the magnetic Green's functions of the capped wedge and cylindrical waveguide given by eqns. 11 and 12, as well as those of the electric type used in the solution of the TM case, and given by eqns. 18 and 24, are valid only for $\rho \geqslant \rho'$ and $\rho' \geqslant \rho$, respectively. The corresponding expressions for $\rho' \geqslant \rho$ and $\rho \geqslant \rho'$ can be obtained by interchanging (ρ, ϕ) and (ρ', ϕ'), i.e. by interchanging the source and field points. The derivations of all these Green's functions are given in [Reference 14 Appendices I and II].

Substituting eqns. 6 and 7 through 10 into the coupled pair of eqns. 3 and 4 gives the following result:

$$\int_{\alpha}^{\pi-\alpha} M_1^h(\phi')(\Gamma^{cw}(a, \phi \,|\, a, \phi') + \varepsilon_r\Gamma^{wg}(a, \phi \,|\, a, \phi'))\, d\phi' + \varepsilon_r \int_{\alpha-\pi}^{-\alpha} M_2^h(\phi')\Gamma^{wg}(a, \phi \,|\, a, \phi')\, d\phi' = -\frac{1}{a}\Gamma^{cw}(\rho_0, \phi_0 \,|\, a, \phi) \quad \pi - \alpha \geqslant \phi \geqslant \alpha \tag{14}$$

$$\varepsilon_r \int_{\alpha}^{\pi-\alpha} M_1^h(\phi')\Gamma^{wg}(a, \phi \,|\, a, \phi')\, d\phi' + \int_{\alpha-\pi}^{-\alpha} M_2^h(\phi') \times (\Gamma^{cw}(a, \phi \,|\, a, \phi') + \varepsilon_r\Gamma^{wg}(a, \phi \,|\, a, \phi'))\, d\phi' = 0 \quad -\alpha \geqslant \phi \geqslant \alpha - \pi \tag{15}$$

4 TM excitation

The source for the TM excitation is an electric line current of unit amplitude. The field produced by this current source can have only a z-component of electric field that does not vary with z and no such component of magnetic field. It then follows from eqns. 1 and 2 that the equivalent magnetic currents have only a ϕ-component that does not vary with z, i.e.

$$M_{1,2}^e = M_{1,2}^e(\phi')a_\phi \tag{16}$$

Thus, the short-circuit field is produced by a z-directed electric line current, while the remaining part of the field in the upper sector, as well as the fields inside the dielectric cylinder and in the lower sector, are produced by ϕ-directed distributions of uniform magnetic line currents. Only of interest, for later application in the continuity eqns. 3 and 4 are the ϕ-components of the magnetic field produced by such currents. The ϕ-component of the short-circuit magnetic field can be derived from a z-directed magnetic vector potential $A^{sc} = A_z^{sc}(\rho, \phi)a_z$ as [Reference 1 Section 5.1]

$$H_\phi^{sc} = -\frac{\partial}{\partial\rho}A_z^{sc}(\rho, \phi) \tag{17}$$

where A_z^{sc} is the same as the electric Green's function $G^{cw}(\rho, \phi \,|\, \rho_0, \phi_0)$ of a capped wedge of half-angle $0.5\pi + \alpha$, where

$$G^{cw}(\rho, \phi \,|\, \rho', \phi') = j\psi(\alpha)\sum_{n=1}^{\infty} H_{n\psi(\alpha)}^{(2)}(\kappa_0 \rho) \times \left(H_{n\psi(\alpha)}^{(2)}(\kappa_0 \rho')\frac{J_{n\psi(\alpha)}(\kappa_0 a)}{H_{n\psi(\alpha)}^{(2)}(\kappa_0 a)} - J_{n\psi(\alpha)}(\kappa_0 \rho')\right) \times \sin n\psi(\alpha)(\phi \mp \alpha)\sin n\psi(\alpha)(\phi' \mp \alpha) \quad \rho \geqslant \rho' \tag{18}$$

The ϕ-components of the magnetic field produced by the magnetic currents can easily be determined with the help of a source equivalence theorem [15]. According to the theorem, ϕ-directed magnetic line currents as given by eqn. 16 produce a magnetic field identical everywhere, except in the source region, with the magnetic field produced by the distribution of electric currents

$$J_{1,2}^e = \frac{1}{j\omega\mu_0\mu_r}\nabla' \times M_{1,2}^e(\phi')\delta(\rho' - a)a_\phi = \frac{1}{j\omega\mu_0\mu_r} M_{1,2}^e(\phi')\frac{\partial}{\partial\rho'}\delta(\rho' - a)a_z \tag{19}$$

where the relative permeability μ_r is unity in the equivalent problems for the upper and lower sectors, and is an arbitrary real constant in the equivalent problem for the dielectric cylinder, and δ is Dirac's 'delta' function. This equivalent distribution is readily recognised as a sheet of z-directed electric line dipoles. The magnetic currents on the short-circuited dielectric interface in the upper sector then produce a magnetic vector potential having only a z-component A_z^u given by

$$A_z^u = \frac{a}{j\omega\mu_0}\int_{\alpha}^{\pi-\alpha} M_1^e(\phi')\int_{a-0}^{a+0} G^{cw}(\rho, \phi \mid \rho', \phi') \times \frac{\partial}{\partial\rho'}\delta(\rho' - a)\, d\rho'\, d\phi'$$
$$= -\frac{a}{j\omega\mu_0}\int_{\alpha}^{\pi-\alpha} M_1^e(\phi')\left(\frac{\partial}{\partial\rho'}G^{cw}(\rho, \phi \mid \rho', \phi')\right)_{\rho'=a} d\phi' \qquad (20)$$

The equality in eqn. 20 is a consequence of the well-known property of the delta function [Reference 16 Section 6.21]

$$\langle f, \delta'\rangle = -\langle f', \delta\rangle \qquad (21)$$

where $\langle ., .\rangle$ signifies an inner product. The ϕ-component of magnetic field produced in the upper sector by the magnetic currents is then given by eqn. 17 with A_z^u replacing A_z^{sc}. Similarly, the ϕ-components of magnetic field produced inside the dielectric cylinder and in the lower sector by the magnetic currents are given by eqn. 17 with A_z^{sc} replaced, respectively, by A_z^d and A_z^l, where

$$A_z^d = \frac{a}{j\omega\mu_0\mu_r}\left(\int_{\alpha}^{\pi-\alpha} \times M_1^e(\phi')\left(\frac{\partial}{\partial\rho'}G^{wg}(\rho, \phi \mid \rho', \phi')\right)_{\rho'=a} d\phi' + \int_{\alpha-\pi}^{-\alpha} M_2^e(\phi')\left(\frac{\partial}{\partial\rho'}G^{wg}(\rho, \phi \mid \rho', \phi')\right)_{\rho'=a} d\phi'\right) \qquad (22)$$

$$A_z^l = -\frac{a}{j\omega\mu_0}\int_{\alpha-\pi}^{-\alpha} \times M_2^e(\phi')\left(\frac{\partial}{\partial\rho'}G^{cw}(\rho, \phi \mid \rho', \phi')\right)_{\rho'=a} d\phi' \qquad (23)$$

In eqn. 22 G^{wg} is the electric Green's function of a cylindrical waveguide

$$G^{wg}(\rho, \phi \mid \rho', \phi') = \frac{1}{j4}\sum_{n=0}^{\infty} \nu_n J_n(\kappa\rho) \times \left(H_n^{(2)}(\kappa\rho') - \frac{H_n^{(2)}(\kappa a)}{J_n(\kappa a)}J_n(\kappa\rho')\right) \times \cos n(\phi - \phi') \quad \rho' \geqslant \rho \qquad (24)$$

Substituting eqns. 17, 20, 22, and 23, into the coupled pair of eqns. 3 and 4 gives the following result:

$$\frac{\partial}{\partial\rho}\int_{\alpha}^{\pi-\alpha} M_1^e(\phi')\left(\frac{\partial}{\partial\rho'}(\mu_r G^{cw}(\rho, \phi \mid \rho', \phi') + G^{wg}(\rho, \phi \mid \rho', \phi'))\right)_{\rho'=a} d\phi' + \frac{\partial}{\partial\rho}\int_{\alpha-\pi}^{-\alpha} M_2^e(\phi')\left(\frac{\partial}{\partial\rho'}G^{wg}(\rho, \phi \mid \rho', \phi')\right)_{\rho'=a} d\phi'$$
$$= \frac{j\omega\mu}{a}\frac{\partial}{\partial\rho}G^{cw}(\rho_0, \phi_0 \mid \rho, \phi) \quad \rho = a, \pi - \alpha \geqslant \phi \geqslant \alpha \qquad (25)$$

$$\frac{\partial}{\partial\rho}\int_{\alpha}^{\pi-\alpha} M_1^e(\phi')\left(\frac{\partial}{\partial\rho'}G^{wg}(\rho, \phi \mid \rho', \phi')\right)_{\rho'=a} d\phi' + \frac{\partial}{\partial\rho}\int_{\alpha-\pi}^{-\alpha} M_2^e(\phi')\left(\frac{\partial}{\partial\rho'}(\mu_r G^{cw}(\rho, \phi \mid \rho', \phi') + G^{wg}(\rho, \phi \mid \rho', \phi'))\right)_{\rho'=a} d\phi' = 0$$
$$\rho = a, \; -\alpha \geqslant \phi \geqslant \alpha - \pi \qquad (26)$$

5 Galerkin's solution

The solution of the coupled pairs of eqns. 14 and 15 in the TE case and eqns. 25 and 26 in the TM case, can readily be carried out using Galerkin's method [Reference 17 Section 1.3]. This is accomplished by expanding the unknown currents in terms of complete sets of orthogonal functions defined on their respective domains. The expansion functions need also be chosen so as to conform with the edge conditions at $\rho = a$, $\phi = \pm\alpha$ and $\pm(\pi - \alpha)$ [Reference 18 Section 1.4]. At the edges of the dented wedges the ϕ-components of the electric field, and hence the magnetic currents for the TE excitation, become infinite, whereas both the z-components of the electric field and the magnetic currents for the TM excitation vanish. Thus, put

$$M_{1,2}^h(\phi') = \sum_{k'=0}^{\infty} a_{1,2k'}^h \cos k'\psi(\alpha)(\phi' \mp \alpha) \qquad (27)$$

$$M_{1,2}^e(\phi') = \sum_{k'=1}^{\infty} a_{1,2k'}^e \sin k'\psi(\alpha)(\phi' \mp \alpha) \qquad (28)$$

Substituting eqn. 27 into eqns. 14 and 15 and testing with $\cos k\psi(\alpha)(\phi \mp \alpha)$, $k = 0, 1, \ldots$, the resulting equations, gives the following system of algebraic equations:

$$\left(\begin{bmatrix} D^h(\alpha) & 0 \\ 0 & D^h(\alpha)\end{bmatrix} + \varepsilon_r\begin{bmatrix} X^h(\alpha) & \tilde{X}^h(\alpha) \\ \tilde{X}^h(\alpha) & X^h(\alpha)\end{bmatrix}\right) \times \begin{bmatrix} a_1^h \\ a_2^h \end{bmatrix} = \begin{bmatrix} b^h(\alpha) \\ 0 \end{bmatrix} \qquad (29)$$

where 0 is the null matrix and D^h and X^h are the matrices

$$D^h(\alpha) = [D_{kk'}^h(\alpha)] = \left[-\frac{1}{\kappa_0 a}\frac{\pi - 2\alpha}{\nu_{k'}}\frac{H_{k'\psi(\alpha)}^{(2)}(\kappa_0 a)}{H_{k'\psi(\alpha)}^{(2)'}(\kappa_0 a)}\delta_{kk'}\right] \qquad (30)$$

$$X^h(\alpha) = [X_{kk'}^h(\alpha)] = \left[\frac{1}{2\pi\kappa a}\sum_{n=0}^{\infty}\nu_n\frac{J_n(\kappa a)}{J_n'(\kappa a)} \times (Cc_{kn}(\alpha)Cc_{k'n}(\alpha) + Cs_{kn}(\alpha)Cs_{k'n}(\alpha))\right] \qquad (31)$$

The elements of $\tilde{X}^h$ and X^h are identical except for a minus sign replacing the plus sign in the bracketed term in eqn. 31. Furthermore, the coefficient vectors a_1^h and a_2^h, and the right-hand side vector b^h, are given by

$$a_1^h = [a_{1,k'}^h] \qquad (32)$$

$$a_2^h = [a_{2,k'}^h] \qquad (33)$$

$$b^h(\alpha) = [b_k^h(\alpha)] = \left[\frac{1}{\kappa_0 a^2}\frac{H_{k\psi(\alpha)}^{(2)}(\kappa_0\rho_0)}{H_{k\psi(\alpha)}^{(2)'}(\kappa_0 a)}\cos k\psi(\alpha)(\phi_0 - \alpha)\right] \qquad (34)$$

while 0 is the null vector. In eqns. 30, 31 and 34 the non-angular factors in the magnetic Green's functions of the capped wedge and cylindrical waveguide are reduced to the forms shown with the help of the Wronskian relationship for the Hankel and Bessel functions [Reference 19 Section 5.9]

$$H_\beta^{(2)\prime}(z)J_\beta(z) - J'_\beta(z)H_\beta^{(2)}(z) = \frac{2}{j\pi z}, \quad \beta, z \in C \tag{35}$$

Furthermore, $\delta_{kk'}$ is Kronecker's 'delta' function (where $\delta_{kk'} = 1$ if $k' = k$, and zero otherwise) and the functions $Cc_{kn}(\alpha)$ and $Cs_{kn}(\alpha)$ are given by

$$\begin{aligned} Cc_{kn}(\alpha) &= \int_\alpha^{\pi-\alpha} \cos k\psi(\alpha)(\phi - \alpha) \cos n\phi \, d\phi \\ &= \frac{n}{n^2 - (k\psi(\alpha))^2} \\ &\quad \times (\cos k\pi \sin n(\pi - \alpha) - \sin n\alpha) \end{aligned} \tag{36}$$

$$\begin{aligned} Cs_{kn}(\alpha) &= \int_\alpha^{\pi-\alpha} \cos k\psi(\alpha)(\phi - \alpha) \sin n\phi \, d\phi \\ &= \frac{-n}{n^2 - (k\psi(\alpha))^2} \\ &\quad \times (\cos k\pi \cos n(\pi - \alpha) - \cos n\alpha) \end{aligned} \tag{37}$$

where, for $\alpha > 0$, $Cc_{00}(\alpha) = \pi - 2\alpha$ and $Cs_{00}(\alpha) = 0$, while for $k, n \neq 0$ they take on the following limiting values:

$$Cc_{kn}(\alpha)\Big|_{n=k\psi(\alpha)} = \tfrac{1}{2}(\pi - 2\alpha)\cos n\alpha - \frac{1}{4n} \times (\sin 3n\alpha + \sin n\alpha) \tag{38}$$

$$Cs_{kn}(\alpha)\Big|_{n=k\psi(\alpha)} = \tfrac{1}{2}(\pi - 2\alpha)\sin n\alpha - \frac{1}{4n} \times (\cos 3n\alpha - \cos n\alpha) \tag{39}$$

Similarly, substituting eqn. 28 into eqns. 25 and 26 and testing with $\sin k\psi(\alpha)(\phi \mp \alpha)$, $k = 1, 2, \ldots$, the resulting equations, gives the following system of algebraic equations:

$$\left(\mu_r \begin{bmatrix} D^e(\alpha) & 0 \\ 0 & D^e(\alpha) \end{bmatrix} + \begin{bmatrix} X^e(\alpha) & \tilde{X}^e(\alpha) \\ \tilde{X}^e(\alpha) & X^e(\alpha) \end{bmatrix}\right) \times \begin{bmatrix} a_1^e \\ a_2^e \end{bmatrix} = \begin{bmatrix} b^e(\alpha) \\ 0 \end{bmatrix} \tag{40}$$

where D^e and X^e are the matrices

$$\begin{aligned} D^e(\alpha) &= [D^e_{kk'}(\alpha)] \\ &= \left[\kappa_0 a \frac{\pi - 2\alpha}{2} \frac{H^{(2)\prime}_{k'\psi(\alpha)}(\kappa_0 a)}{H^{(2)}_{k'\psi(\alpha)}(\kappa_0 a)} \delta_{kk'}\right] \end{aligned} \tag{41}$$

$$\begin{aligned} X^e(\alpha) &= [X^e_{kk'}(\alpha)] \\ &= \left[-\frac{\kappa a}{2\pi} \sum_{n=0}^{\infty} v_n \frac{J'_n(\kappa a)}{J_n(\kappa a)} \right. \\ &\quad \left. \times (Ss_{kn}(\alpha)Ss_{k'n}(\alpha) + Sc_{kn}(\alpha)Sc_{k'n}(\alpha))\right] \end{aligned} \tag{42}$$

Likewise, the elements of $\tilde{X}^e$ and X^e are identical, except for a minus sign replacing the plus sign in the bracketed term in eqn. 42, while the coefficient vectors a_1^e and a_2^e, and the right-hand side vector b^e, are given by

$$a_1^e = [a^e_{1,k'}] \tag{43}$$

$$a_2^e = [a^e_{2,k'}] \tag{44}$$

$$\begin{aligned} b^e(\alpha) &= [b^e_k(\alpha)] \\ &= \left[j\omega\mu \frac{H^{(2)}_{k\psi(\alpha)}(\kappa_0 \rho_0)}{H^{(2)}_{k\psi(\alpha)}(\kappa_0 a)} \sin k\psi(\alpha)(\phi_0 - \alpha)\right] \end{aligned} \tag{45}$$

Again, the Wronskian relationship (eqn. 35) is utilised to reduce the nonangular parts of $(\partial^2/\partial\rho\,\partial\rho')G^{cw}$ and $(\partial^2/\partial\rho\,\partial\rho')G^{wg}$, $\rho = \rho' = a$, and of $(\partial/\partial\rho)G^{cw}$, $\rho = a$, to the forms shown in eqns. 41, 42 and 45, respectively. Furthermore, the functions $Sc_{kn}(\alpha)$ and $Ss_{kn}(\alpha)$ in eqn. 42 are given by

$$\begin{aligned} Ss_{kn}(\alpha) &= \int_\alpha^{\pi-\alpha} \sin k\psi(\alpha)(\phi - \alpha) \sin n\phi \, d\phi \\ &= \frac{k\psi(\alpha)}{n^2 - (k\psi(\alpha))^2} \\ &\quad \times (\cos k\pi \sin n(\pi - \alpha) - \sin n\alpha) \end{aligned} \tag{46}$$

$$\begin{aligned} Sc_{kn}(\alpha) &= \int_\alpha^{\pi-\alpha} \sin k\psi(\alpha)(\phi - \alpha) \cos n\phi \, d\phi \\ &= \frac{k\psi(\alpha)}{n^2 - (k\psi(\alpha))^2} \\ &\quad \times (\cos k\pi \cos n(\pi - \alpha) - \cos n\alpha) \end{aligned} \tag{47}$$

where $Ss_{kn}(\alpha)$ and $Sc_{kn}(\alpha)$ take on the following limiting values for $\alpha > 0$

$$Ss_{kn}(\alpha)\Big|_{n=k\psi(\alpha)} = \tfrac{1}{2}(\pi - 2\alpha)\cos n\alpha + \frac{1}{4n} \times (\sin 3n\alpha + \sin n\alpha) \tag{48}$$

$$Sc_{kn}(\alpha)\Big|_{n=k\psi(\alpha)} = -\tfrac{1}{2}(\pi - 2\alpha)\sin n\alpha - \frac{1}{4n} \times (\cos 3n\alpha - \cos n\alpha) \tag{49}$$

The solutions of the systems of eqns. 29 and 40 determine the expansion coefficients of the equivalent magnetic currents on the dielectric interfaces, hence the complete field solutions for the TE and TM excitations, respectively. It is worth noting that if the parameters of the dielectric cylinder are so chosen that κa is around the mth root of the Bessel function J_n in eqn. 42, or its derivative in eqn. 31, then the field in the dielectric cylinder is basically that of the TM_{nm}, or TE_{nm}, to z mode in a perfectly conducting cylindrical waveguide of the same medium and radius. In this case the nth terms of the series in eqns. 31 and 42 become dominant and can therefore be used to approximate the series, thereby substantially reducing the amount of work involved in the solution.

6 Transmitted field and power

The field transmitted into the lower sector can easily be determined in terms of the magnetic currents M_2^h and M_2^e. Substituting eqns. 10, 11 and 27 into eqn. 6, the transmitted magnetic field for the TE excitation is readily found to be given by

$$H_z^l = j\frac{1}{\eta_0} \sum_{k'=0}^{\infty} a^h_{2,k'} \frac{H^{(2)}_{k'\psi(\alpha)}(\kappa_0 \rho)}{H^{(2)\prime}_{k'\psi(\alpha)}(\kappa_0 a)} \cos k'\psi(\alpha)(\phi + \alpha) \tag{50}$$

where η_0 is the free space wave impedance. Similarly, the transmitted electric field for the TM excitation has only a z-component given by [Reference 1 Section 5.1]

$$E_z^l = -j\omega\mu_0 A_z^l(\rho, \phi) \tag{51}$$

which, upon using eqns. 18, 23 and 28, becomes

$$E_z^l = \sum_{k'=1}^{\infty} a_{2,k'}^e \frac{H_{k'\psi(\alpha)}^{(2)}(\kappa_0 \rho)}{H_{k'\psi(\alpha)}^{(2)}(\kappa_0 a)} \sin k'\psi(\alpha)(\phi + \alpha) \tag{52}$$

The complex power transmitted into the lower sector is of interest as well. The complex power transmitted into the lower sector just beyond $\rho = a$ for the TE excitation is basically

$$P_t^h = -a \int_{\alpha-\pi}^{-\alpha} M_2^h H_z^{l*}(M_2^h)\, d\phi' \tag{53}$$

where the asterisk '*' denotes complex conjugate. Using eqns. 27 and 50, eqn. 53 becomes

$$P_t^h = j \frac{a}{\eta_0} \sum_{k=0}^{\infty} \sum_{k'=0}^{\infty} a_{2,k}^h \frac{\pi - 2\alpha}{\nu_{k'}} \times \left(\frac{H_{k'\psi(\alpha)}^{(2)}(\kappa_0 a)}{H_{k'\psi(\alpha)}^{(2)\prime}(\kappa_0 a)} \right)^* \delta_{kk'} a_{2,k'}^{h*} \tag{54}$$

which can be put in the matrix form

$$P_t^h = -j \frac{\kappa_0}{\eta_0} a^2 a_2^{hT} D^{h*}(\alpha) a_2^{h*} \tag{55}$$

where the superscript 'T' denotes vector transpose. Similarly, the complex power transmitted into the lower sector for the TM excitation just beyond $\rho = a$ is given by

$$P_t^e = -a \int_{\alpha-\pi}^{-\alpha} M_2^e H_\phi^{l*}(M_2^e)\, d\phi' \tag{56}$$

Substituting eqns. 17, 23 and 28 into eqn. 56 results in the following:

$$P_t^e = -j \frac{a}{2\eta_0} \sum_{k=1}^{\infty} \sum_{k'=1}^{\infty} a_{2,k}^e (\pi - 2\alpha) \left(\frac{H_{k'\psi(\alpha)}^{(2)\prime}(\kappa_0 a)}{H_{k'\psi(\alpha)}^{(2)}(\kappa_0 a)} \right)^* \delta_{kk'} a_{2,k'}^{e*}$$
$$= -j \frac{1}{\kappa_0 \eta_0} a_2^{eT} D^{e*}(\alpha) a_2^{e*} \tag{57}$$

The time-average power transmitted into the lower sector can be obtained from the transmitted complex power according to [Reference 1 Section 1.10]

$$\langle P_t \rangle = \mathrm{Re}\,(P_t) \tag{58}$$

where Re (P) denotes the real part of $P \in C$. Thus, substituting eqn. 54 for P_t^h, and eqn. 57 for P_t^e into eqn. 58, and using the Wronskian relationship (eqn. 35), the time-average powers transmitted into the lower sector, respectively, for the TE and TM excitations are readily found to be

$$\langle P_t^h \rangle = \frac{1}{\kappa_0 \eta_0 \psi(\alpha)} \sum_{k'=0}^{\infty} \frac{2}{\nu_{k'}} \left| \frac{a_{2,k'}^h}{H_{k'\psi(\alpha)}^{(2)\prime}(\kappa_0 a)} \right|^2 \tag{59}$$

$$\langle P_t^e \rangle = \frac{1}{\kappa_0 \eta_0 \psi(\alpha)} \sum_{k'=1}^{\infty} \left| \frac{a_{2,k'}^e}{H_{k'\psi(\alpha)}^{(2)}(\kappa_0 a)} \right|^2 \tag{60}$$

7 Transmission coefficient

A parameter conveniently characterising the penetration of electromagnetic field into the lower sector is the transmission coefficient. By definition [Reference 1 Section 7.12], the transmission coefficient T of the dielectric-loaded double dented wedge is the ratio of the time-average power transmitted through the dielectric interface at $\rho = a$, $-\alpha \geqslant \phi \geqslant \alpha - \pi$, into the lower sector to the time-average power produced by the line current source.

The time-average power produced by the line current source is basically

$$\langle P_i \rangle = \mathrm{Re}\,(P_i) \tag{61}$$

where P_i is the complex power produced by the line current source in free space. The time-average power produced by the magnetic line current for the TE excitation is then given by

$$\langle P_i^h \rangle = -\mathrm{Re} \int_0^{2\pi} H_i^h \frac{1}{\rho} \delta(\rho - \rho_0)\delta(\phi - \phi_0) \rho\, d\phi \tag{62}$$

where H_i^h is the magnetic field produced by a magnetic line current of unit strength in free space, i.e.

$$H_i^h = -\frac{\kappa_0}{4\eta_0} H_0^{(2)}(\kappa_0 |\rho - \rho_0|)$$
$$= -\frac{\kappa_0}{4\eta_0} \sum_{n=0}^{\infty} \nu_n J_n(\kappa_0 \rho) H_0^{(2)}(\kappa_0 \rho_0) \cos n(\phi - \phi_0)$$
$$\rho < \rho_0 \tag{63}$$

The equality in eqn. 63 is a statement of the addition theorem for the Hankel function of the second kind and zeroth order [Reference 1 Section 5.8]. Substituting eqn. 63 into eqn. 62, and using the identity 9.1.76 of Reference 20 gives

$$J_0^2(z) + 2 \sum_{n=1}^{\infty} J_n^2(z) = 1 \quad z \in C \tag{64}$$

the time-average power produced by the magnetic line current in free space for the TE excitation is readily found to be

$$\langle P_i^h \rangle = \frac{\kappa_0}{4\eta_0} \tag{65}$$

The time-average power produced by the electric line current in free space for the TM excitation can be obtained in a similar fashion, or more simply, by using duality [Reference 1 Section 3.2] as follows:

$$\langle P_i^e \rangle = \tfrac{1}{4} \kappa_0 \eta_0 \tag{66}$$

Finally, using eqns. 59, 60, 65 and 66 the transmission coefficients T^h and T^e, respectively, for the TE and TM excitations become

$$T^h = \frac{4}{\kappa_0^2 \psi(\alpha)} \sum_{k'=0}^{\infty} \frac{2}{\nu_{k'}} \left| \frac{a_{2,k'}^h}{H_{k'\psi(\alpha)}^{(2)\prime}(\kappa_0 a)} \right|^2 \tag{67}$$

$$T^e = \frac{4}{\kappa_0^2 \eta_0^2 \psi(\alpha)} \sum_{k'=1}^{\infty} \left| \frac{a_{2,k'}^e}{H_{k'\psi(\alpha)}^{(2)}(\kappa_0 a)} \right|^2 \tag{68}$$

8 Specialisation to dielectric-loaded slit

The analysis of the dielectric-loaded double dented wedge structure can be specialised to the problem of a slit loaded with a dielectric cylinder. Evidently, the specialisation is immediately realised by setting $\alpha = 0$.

The solution of the problem of the dielectric-loaded slit can then be obtained by solving the systems of eqns. 29 and 40 with α set equal to zero. In this case, only Bessel and Hankel functions of integral orders are involved in the Galerkin's matrices. Furthermore, the functions $Cc_{kn}(0)$ and $Cs_{kn}(0)$ for the TE excitation and

$Ss_{kn}(0)$ and $Sc_{kn}(0)$ for the TM excitation become

$$Cc_{kn}(0) = \frac{\pi}{\nu_k}\,\delta_{kn} \tag{69}$$

$$Cs_{kn}(0) = Sc_{nk}(0) = \begin{cases} 0, & \text{for } n = k \\ \dfrac{n}{n^2 - k^2}(1 - \cos k\pi \cos n\pi), & \text{for } n \neq k \end{cases} \tag{70}$$

$$Ss_{kn}(0) = \frac{\pi}{2}\,\delta_{kn} \tag{71}$$

The field and power transmitted into the lower sector, as well as transmission coefficients, are given by the formulas of the previous two Sections with α set equal to zero.

9 Plane wave excitation

As has already been indicated the case of plane wave excitation can be treated by letting the line sources recede to infinity. The solutions for TE and TM plane wave excitation are then readily obtained by replacing the Hankel functions in the right-hand side vectors b^h and b^e by their large argument approximation [Reference 19 Section 5.11], i.e.

$$H^{(2)}_{k\psi(\alpha)}(\kappa_0 \rho_0) \simeq \sqrt{\left(j\frac{2}{\pi\kappa_0\rho_0}\right)}\, j^{k\psi(\alpha)} e^{-j\kappa_0\rho_0} \tag{72}$$

Furthermore, for the z-component of field of the incident plane wave to be of unit amplitude, the following normalisation is utilized:

$$G\sqrt{\left(j\frac{2}{\pi\kappa_0\rho_0}\right)} e^{-j\kappa_0\rho_0} = 1 \tag{73}$$

where

$$G = \begin{cases} -\dfrac{1}{4\eta_0}\kappa_0 & \text{for TE plane wave} \\ -\dfrac{1}{4}\kappa_0\eta_0 & \text{for TM plane wave} \end{cases} \tag{74}$$

The solutions of the systems of eqns. 29 and 40 with the right-hand side vectors modified according to eqns. 72 to 74 determine the expansion coefficients of the equivalent magnetic currents on the dielectric interfaces of the dielectric-loaded double dented wedge structure when excited, respectively, by TE and TM plane waves of unit amplitude. The electromagnetic field and power transmitted into the lower sector are still given by the formulas in Section 6. Only the transmission coefficients need to be modified. Specifically, since the time-average power incident is $1/\eta_0$ for a TE plane wave of unit amplitude and η_0 for a TM plane wave of unit amplitude, the transmission coefficients become

$$T^h = \frac{1}{\kappa_0 \eta_0^2 \psi(\alpha)} \sum_{k'=0}^{\infty} \frac{2}{\nu_{k'}} \left| \frac{a^h_{2,k'}}{H^{(2)\prime}_{k'\psi(\alpha)}(\kappa_0 a)} \right|^2 \tag{75}$$

$$T^e = \frac{1}{\kappa_0 \psi(\alpha)} \sum_{k'=1}^{\infty} \left| \frac{a^e_{2,k'}}{H^{(2)}_{k'\psi(\alpha)}(\kappa_0 a)} \right|^2 \tag{76}$$

10 Numerical results

The analysis presented has been implemented in the form of a computer program. Only a sample of the results obtained for the problems of two dented wedges and a slit, loaded with a nonmagnetic ($\mu_r = 1.0$) dielectric cylinder and excited by a plane wave are presented here. More results can be found in Reference 14.

The actual solution of the problem involves determining the order of the Galerkin's matrices or the number of orthogonal functions needed in the expansions of the currents. These latter numbers have simply been determined as the indices of the first elements of the right-hand side vectors b^h and b^e of magnitude less than 10^{-12}. To this end convergence tests for a wide range of parameter values have been conducted and the number of orthogonal functions needed for the convergence of the solution has been found to conform with the adopted policy. An example of the convergence characteristics of the solution is shown in Fig. 4 for the transmission coefficients for the unloaded slit ($\varepsilon_r = 1.0$) for $\kappa_0 a = 0.5$, 5.0 and 10.0 in the case of normally incident TE and TM plane waves. As can be seen only a few expansion functions are needed even for large values of $\kappa_0 a$. The stair-like behaviour displayed in Fig. 4 can be attributed to the fact that for $\alpha = 0$, every other element in the right-hand vectors b^h and b^e is zero.

Furthermore, as a check of the accuracy of the solution, the results obtained for the unloaded slit have been compared with the exact solution of Skavlem [4]. The

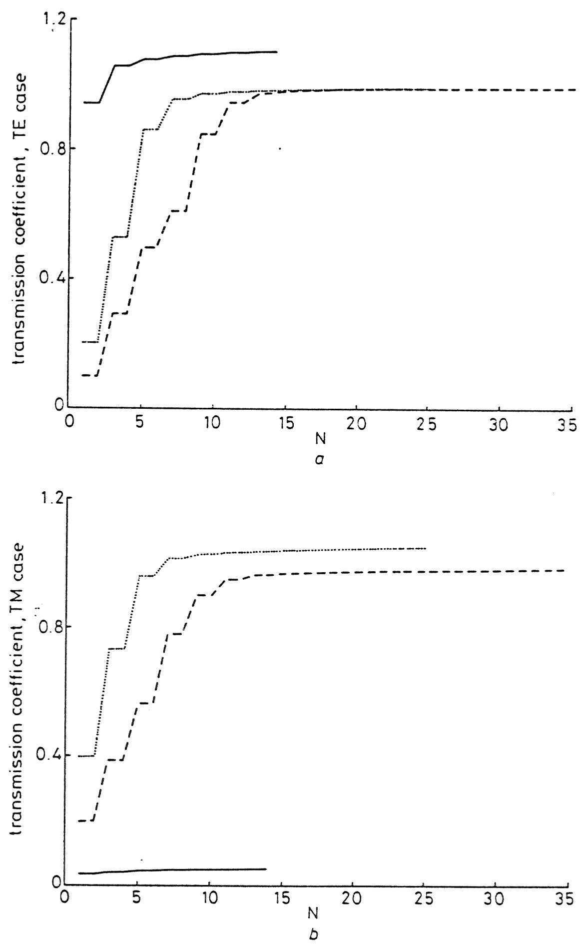

Fig. 4 *Convergence characteristics of transmission coefficient for unloaded slit in the case of normal incidence as number of expansion functions increases*

a TE excitation
b TM excitation
——— $\kappa_0 a = 0.5$
······ $\kappa_0 a = 5.0$
- - - - $\kappa_0 a = 10.0$

agreement between the two sets of data has been found to be excellent, as can be inferred from Fig. 5. The changes of the transmission coefficients for the dielectric-loaded slit with frequency for $\varepsilon_r = 1.0$, 5.0 and 9.0 and with dielectric constant for $\kappa_0 a = 0.5$, 1.0 and 1.5 in the case of normal incidence are shown in Figs. 5 and 6, respectively. In Fig. 5 data has been collected for values of $\kappa_0 a$ up to 10.0, but no plots of the data are given in the region $6.0 < \kappa_0 a < 10.0$, as their rapidly increasing oscillations make it difficult to distinguish between them. It is worth mentioning that the results obtained for the loaded slit have also been compared with the quasistatic solution for the TM excitation by Hurd and Sachdeva [21] with equal success. For instance, an examination of Fig. 5*b* shows that the first three resonances for the TM excitation occur at $2\kappa a = 2.7$, 4.5 and 7.65 for $\varepsilon_r = 9.0$, compared to 2.7, 4.5 and 7.6 as determined by Hurd and Sachdeva.

The changes of the transmission coefficients with $\kappa_0 a$ for different values of α for the dielectric-loaded double dented wedge are shown in Fig. 7 for $\varepsilon_r = 1.0$ in the case of normal incidence, whereas the corresponding transmitted far field patterns are shown in Fig. 8 for $\kappa_0 a = 5.0$. Here, it is important to recall that $\alpha = 0$ corresponds to the unloaded slit problem. As can be seen, the wedge angle does not have a pronounced effect on the transmission coefficient for either excitation. Furthermore, the transmission coefficients for $\alpha = 15°$ and 30° and $\kappa_0 a > 6$ are always less than the geometrical optics value of unity for any two wedges of large separation [5, 11]. On the other hand, the beamwidth of the transmitted far field patterns oscillates as the wedge angle is increased. Also, in the case of TM excitation, the pattern for $\alpha = 15°$, 30° and 45° is characterised by a single beam that almost covers the whole lower sector. Finally, the transmitted far field patterns for a dielectric-loaded double dented wedge of half-angle $\alpha = 25°$ for $\kappa_0 a = 7.0$ and $\varepsilon_r = 1.0$, 5.0 and 9.0 in the case of normal incidence, and for $\kappa_0 a = 7.0$ and $\varepsilon_r = 5.0$ for different angles of incidence are shown in Figs. 9 and 10, respectively.

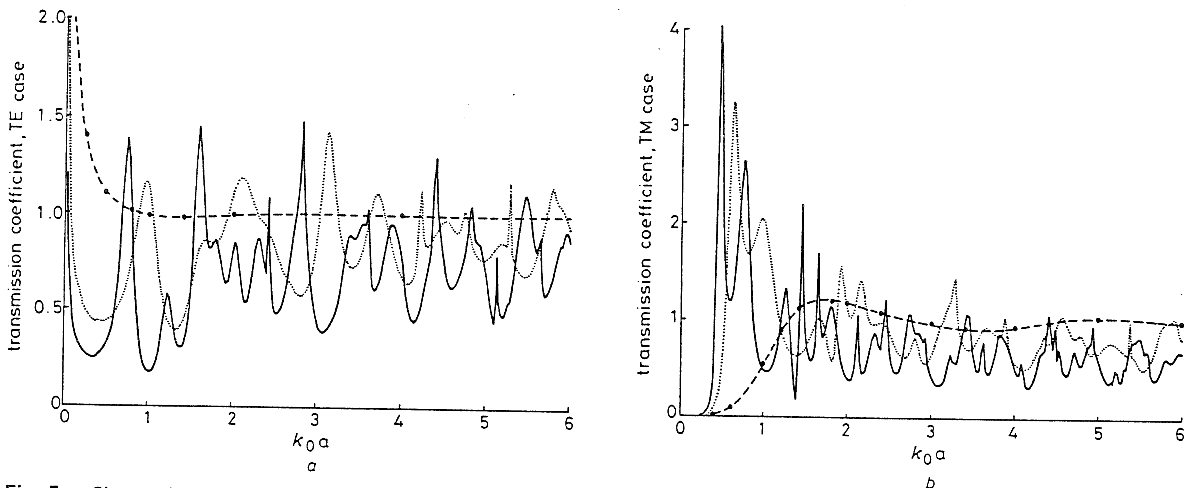

Fig. 5 *Change of transmission coefficient for loaded slit with $\kappa_0 a$ in the case of normal incidence*
a TE excitation
b TM excitation
- - - - $\varepsilon_r = 1.0$ (••• exact solution [4])
······ $\varepsilon_r = 5.0$ ——— $\varepsilon_r = 9.0$

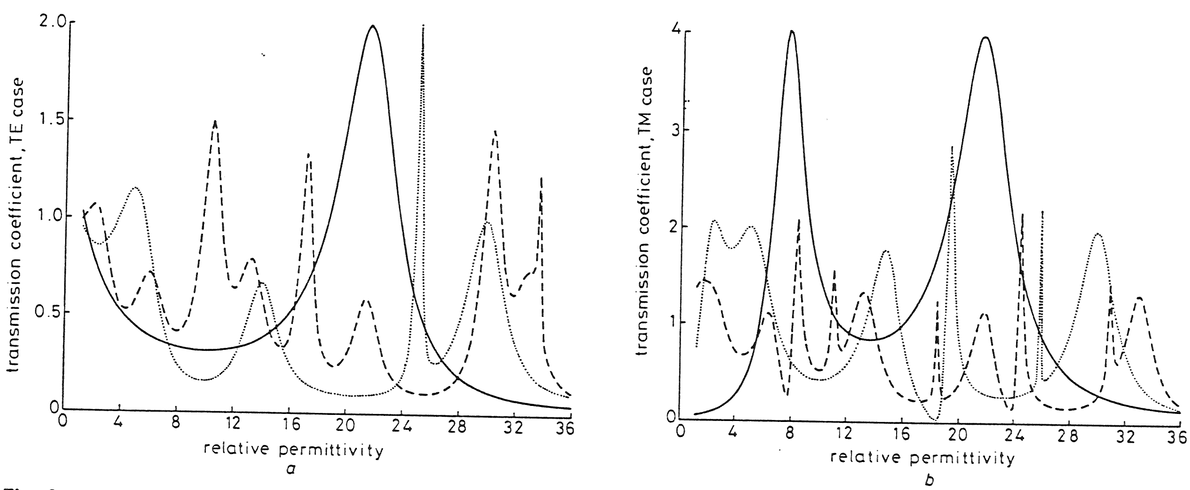

Fig. 6 *Change of transmission coefficient for loaded slit with ε_r in the case of normal incidence*
a TE excitation
b TM excitation
——— $\kappa_0 a = 0.5$
······ $\kappa_0 a = 1.0$
- - - - $\kappa_0 a = 1.5$

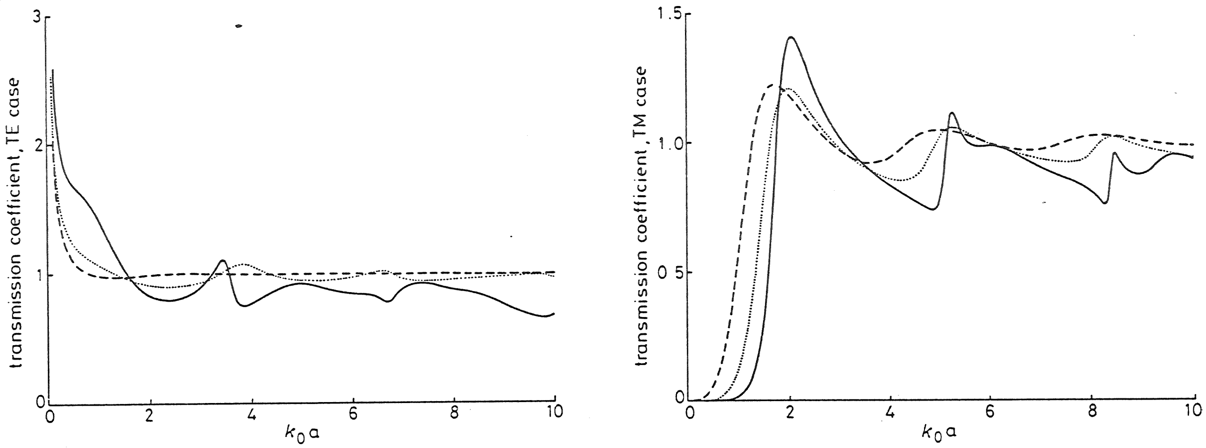

a b

Fig. 7 *Change of transmission coefficient for unloaded double dented wedge with $\kappa_0 a$ in the case of normal incidence*
a TE excitation *b* TM excitation
——— $\alpha = 0°$ ······· $\alpha = 15°$ – – – – $\alpha = 30°$

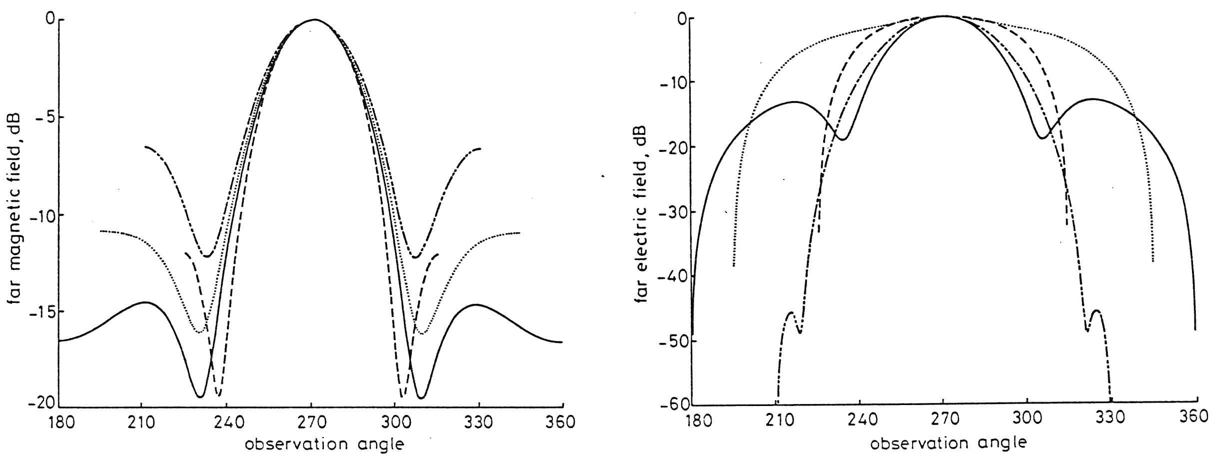

a b

Fig. 8 *Transmitted far field pattern for unloaded double dented wedge in the case of normal incidence for $\kappa_0 a = 5.0$*
a TE excitation *b* TM excitation
——— $\alpha = 0°$ ······· $\alpha = 15°$ —·· — $\alpha = 30°$ – – – – $\alpha = 45°$

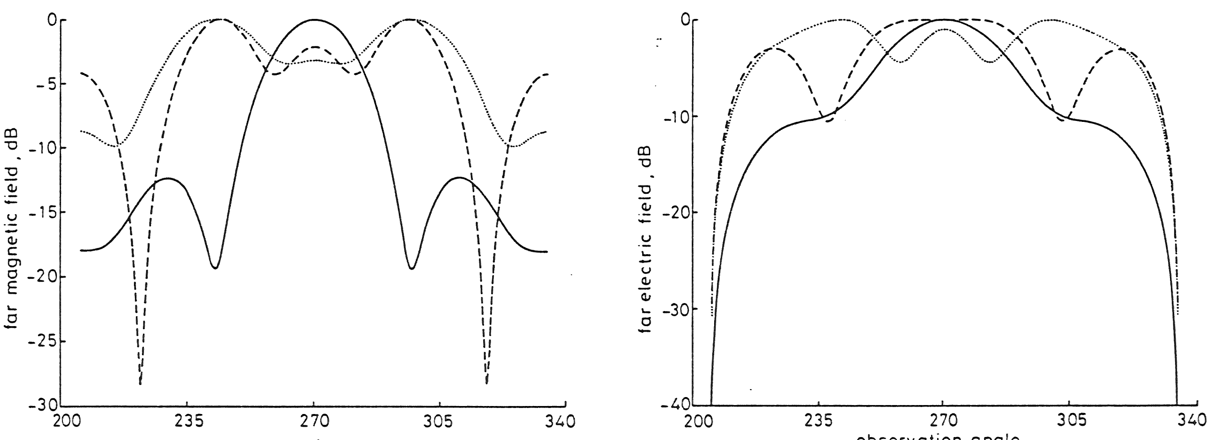

a b

Fig. 9 *Transmitted far field pattern for dielectric-loaded double dented wedge $\alpha = 25°$ in the case of normal incidence for $\kappa_0 a = 7.0$*
a TE excitation *b* TM excitation
——— $\varepsilon_r = 1.0$ ······· $\varepsilon_r = 5.0$ – – – – $\varepsilon_r = 9.0$

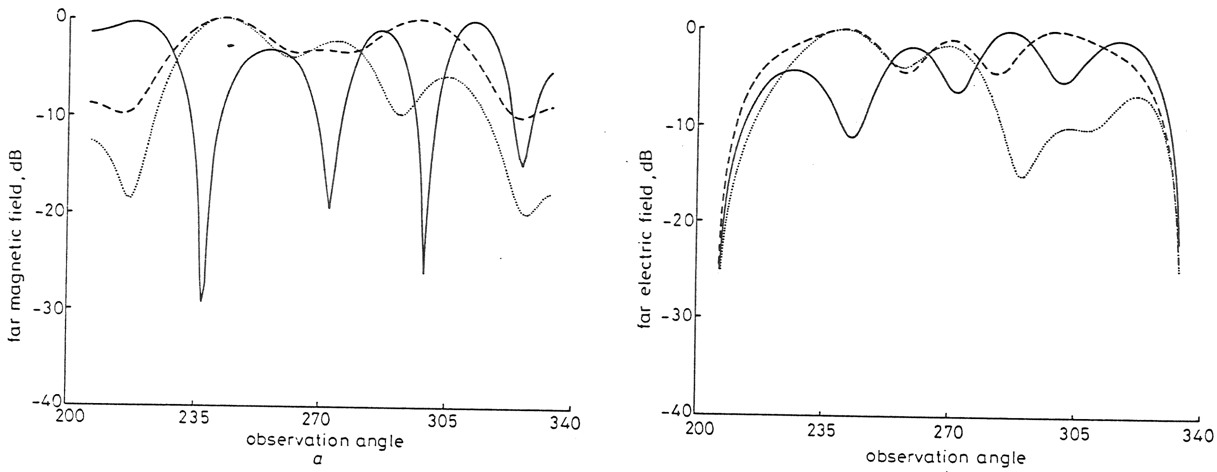

Fig. 10 *Transmitted far field pattern for dielectric-loaded double dented wedge $\alpha = 25°$, for $\kappa_0 a = 7.0$ and $\varepsilon_r = 5.0$*
a TE excitation
b TM excitation
——— $\phi_0 = 30°$
······ $\phi_0 = 60°$
- - - - $\phi_0 = 90°$

11 Summary

A rigorous field analysis of the problem of two identical perfectly conducting parallel wedges with dented edges loaded with a dielectric cylinder has been given in this paper for both TE and TM excitations. The analysis has then been specialised to the problem of a dielectric-loaded slit. Numerical results for the two problems have also been given in the case of plane wave excitation.

12 References

1 HARRINGTON, R.F.: 'Time-harmonic electromagnetic fields' (McGraw-Hill Book Company, New York, USA, 1961)
2 NUSSENZVEIG, H.M.: 'Solution of a diffraction problem, I. the wide double wedge', *Philos. Trans. R. Soc. Lon.*, 1959, **252**, pp. 1–30
3 NUSSENZVEIG, H.M.: 'Solution of a diffraction problem, II. the narrow double wedge', *ibid.*, 1959, **252**, pp. 31–5130
4 SKAVLEM, S.: 'On the diffraction of scalar plane waves by a slit of infinite length', *Arch. Math. Naturvidenskab*, 1952, **51**, pp. 61–80
5 TEAGUE, B.R., and ZITRON, N.R.: 'Diffraction by an aperture between two wedges', *Appl. Sci. Res.*, 1972, **26**, pp. 127–137
6 ZITRON, N.R., and KARP, S.N.: 'Higher order approximation in multiple scattering, I. two-dimensional scalar case', *J. Math. Phys.*, 1961, **2**, pp. 394–402
7 ELSHERBENI, A.Z., and HAMID, M.: 'Diffraction by a wide double wedge', *IEEE Trans.*, 1984, **AP-32**, pp. 1262–1265
8 KARP, S.N., and RUSSEK, A.: 'Diffraction by a wide slit', *J. Appl. Phys.*, 1956, **27**, pp. 886–894
9 ELSHERBENI, A.Z., and HAMID, M.: 'Novel cylindrical-wave spectrum for analysis of scattering by multiple bodies', *IEE Proceedings, H, Microwaves, Antenna & Propag.*, 1987, **134**, pp. 35–44
10 ELSHERBENI, A.Z., and HAMID, M.: 'Diffraction by a wide double wedge with rounded edges', *IEEE Trans.*, 1985, **AP-33**, pp. 1012–1015
11 ELSHERBENI, A.Z., and HAMID, M.: 'Diffraction by a wide double wedge with capped edges', *ibid.*, 1986, **AP-34**, pp. 947–951
12 ELSHERBENI, A.Z., and HAMID, M.: 'Scattering by a double wedge and a parallel cylinder', *Int. J. Electron.*, 1986, **60**, pp. 367–380
13 ELSHERBENI, A.Z., and HAMID, M.: 'Diffraction properties of a class of double wedges', *Can. J. Phys.*, 1987, **65**, pp. 16–22
14 ELSHERBENI, A.Z., and AUDA, H.A.: 'Electromagnetic diffraction by two perfectly conducting wedges with dented edges loaded with a dielectric cylinder'. Technical Report, Department of Electrical Engineering, University of Mississippi, November 1988
15 MAYES, P.E.: 'The equivalence of electric and magnetic sources', *IRE Trans.*, 1985, **AP-6**, pp. 295–296
16 KOLMOGOROV, A.N., and FOMIN, S.V.: 'Introductory real analysis' (Dover Publications, Inc., New York, USA, 1970)
17 HARRINGTON, R.F.: 'Field computation by moment methods' (Macmillan Company, New York, USA, 1968, reprinted by Krieger Publishing Company, Melbourne, Florida, USA, 1982)
18 COLLIN, R.E.: 'Field theory of guided waves' (McGraw-Hill Book Company, New York, USA, 1960)
19 LEBEDEV, N.N.: 'Special functions and their applications', SILVERMAN R.A., (Ed.): (Dover Publications, Inc., New York, 1972)
20 ABRAMOWITZ, M., and STEGUN, I.A.: 'Handbook of mathematical functions' (Dover Publications, Inc., New York, 1970)
21 HURD, R.A., and SACHDEVA, B.K.: 'Scattering by a dielectric-loaded slit in a conducting plane', *Rad. Sci.*, 1975, **10**, pp. 565–572